Imperfections of the Thermohaline Circulation: Multiple Equilibria and Flux Correction*

HENK A. DIJKSTRA

Institute for Marine and Atmospheric Research Utrecht, Utrecht University, Utrecht, the Netherlands

J. DAVID NEELIN

Department of Atmospheric Sciences and Institute of Geophysics and Planetary Physics, University of California, Los Angeles, Los Angeles, California

(Manuscript received 20 June 1997, in final form 8 June 1998)

ABSTRACT

Within one of the simplest models that represents thermohaline transport in the ocean, a two-dimensional Boussinesq model under mixed boundary conditions, the relationship between multiple equilibria in a flux-corrected model and an uncorrected model is considered. Flux-correction procedures are used in some climate models to maintain a climate state close to observed, compensating for model errors by introducing artificial fluxes between model components. A correction procedure used in many ocean or ocean–atmosphere models of the thermohaline circulation involves calculating the freshwater flux required to maintain observed surface salinity and then specifying this flux. In the prototype system here, one model solution is chosen as the ''true'' solution and flux correction is applied to model versions with different parameters. When the flux correction is not too large, it is qualitatively successful, particularly in reproducing the equilibrium state for which the correction is designed. However, other equilibria are more strongly affected, and the connections between equilibria are changed. Furthermore, areas in parameter space exist with multiple equilibria in the flux-corrected case that have a unique state in the uncorrected case. Care should thus be used in drawing conclusions on the existence of multiple equilibria and the stability of the thermohaline circulation when a flux-correction procedure is used. Guidelines are provided to help distinguish spurious equilibria in a flux-corrected model. The computation of an uncorrected equilibrium is useful, even if it does not resemble observations.

1. Introduction

Since the work of Stommel (1961), Broecker et al. (1985), and Bryan (1986), it has been recognized that there may exist multiple equilibria of the global thermohaline circulation. An important motivation for this work is to determine whether the present ocean circulation is easily perturbed, for example, through relatively small surface freshwater flux perturbations, to give large changes in circulation associated with changing to another equilibrium state.

Multiple equilibria and transitions between these equilibria have been found in a hierarchy of ocean models, ranging from simple box models (Stommel 1961) to global oceanic general circulation models (OGCMs; Weaver and Hughes 1992, and references therein). Central to these results is the issue of mixed surface boundary conditions; that is, while surface temperature is prescribed or restored toward a given function of space, the freshwater flux at the ocean–atmosphere surface is largely independent of the sea surface salinity. In single basin OGCMs, three states were distinguished under symmetric surface forcing: two pole-to-pole circulations and one symmetric thermally driven circulation (Bryan 1986).

Simpler models have shown that one of the origins of multiple equilibria is a meridional advective feedback mechanism. The mechanism is shown in its purest form in the case of an equatorially symmetric setup, where it is associated with a symmetry breaking pitchfork bifurcation (Thual and McWilliams 1992; Quon and Ghil 1992). For sufficiently large thermal forcing, a symmetric state with downwelling at the poles is unique at weak haline forcing. At the pitchfork, this symmetric state becomes unstable to asymmetric perturbations as described in detail in Dijkstra and Molemaker (1997). The instability leads to the existence of stable pole-to-

* University of California, Los Angeles, Institute of Geophysics and Planetary Physics Publication Number 4890.

Corresponding author address: Dr. Henk A. Dijkstra, Institute for Marine and Atmospheric Research Utrecht, Utrecht University, 3508TA Utrecht, the Netherlands.
E-mail: dijkstra@fys.ruu.nl

pole solutions. Because of the internal reflection symmetry, both southward sinking and northward sinking branches occur.

Since this mechanism of the occurrence of multiple equilibria is so robust within a hierarchy of models, one may conjecture that the details of the momentum balance are not important as long as the meridional advective feedback is represented. Consequently, to study the structure of multiple equilibria originating from this symmetry breaking mechanism, relatively simple models can be used (see, e.g., Marotzke 1994). It should be noted, however, that the temporal transitions between the different states still depend strongly on the type of model used. For example, the transients between two states may be quite different in two-dimensional and three-dimensional models, because processes with quite different timescales are represented. In addition, the advective feedback may not be the only source of multiple equilibria. Multiple equilibria have also been found associated with localized sites of convection (Rahmstorf 1994; Lenderink and Haarsma 1994).

Although mixed boundary conditions are physically reasonable because the sea surface salinity has no direct feedback on the freshwater flux, a serious drawback is that the atmosphere is treated as a passive component. Hence, the issues of multiple equilibria, as found in OGCMs using mixed boundary conditions, need reexamination in a coupled context. First steps have been taken by Zhang et al. (1993), Marotzke and Stone (1995), and more recently by Saravanan and McWilliams (1995). In the last study, it was shown that within an intermediate coupled ocean–atmosphere model, the multiple equilibria resulting from the oceanic advective feedback persist in a coupled model. Although there is a major effort in the development of globally coupled GCMs, at the moment most of these models still suffer from climate drift due to mismatches in balances between certain components of the coupled system (Moore and Gordon 1994). In many models, this drift is overcome by using an artificial correction to maintain the mean state near a desired state. This procedure is known as ''flux correction'' (Sausen et al. 1988) or ''flux adjustment'' (Manabe and Stouffer 1988).

This study is motivated by the results in Manabe and Stouffer (1988, MS88 hereafter) who found two different equilibria in a coupled climate model, using flux correction. In a preliminary run with their coupled model, the integration starts from an isothermal, dry atmosphere and an isothermal, isohaline ocean with both at rest. After 1000 (upper ocean) yr, the trajectory reaches an equilibrium, which we will refer to as E_p. In this case, the overturning circulation is much too weak in the North Atlantic, leading to erroneous salt and sea surface temperature fields. From this state, they continue the integration but with sea surface salinity restored strongly toward a specified observed field. During the integration to a new equilibrium, say E_r, they determine the freshwater flux necessary to maintain this surface salinity field within this equilibrium. This freshwater flux is then used in the flux-corrected experiments. The two different equilibria, say E_1 and E_2, in the coupled model are obtained by starting integrations at E_p and E_r using the flux adjustment within the coupled model. The difference between the two equilibria is particularly notable in the rate of North Atlantic Deep Water formation.

In studying multiple equilibria, it is often useful to compute solutions as a function of parameters and to examine the relationship between the various solution branches in parameter space. Such bifurcation structures for the thermohaline circulation in two-dimensional models under latitudinally symmetric boundary conditions have been inferred from time integrations (Thual and McWilliams 1992; Quon and Ghil 1992) and computed directly using continuation methods (Dijkstra and Molemaker 1997). Although the ''true'' system is normally conceptualized as having one particular set of values of the parameters, knowing the behavior through a range of parameters gives information about the robustness of qualitative behavior against uncertainty in parameter choices. ''Imperfection theory'' is sometimes used to denote the aspects of bifurcation theory that classify how qualitative connections between solution regimes change when symmetries or other restrictions on external conditions upon a dynamical system give way to more general conditions. Using continuation techniques and imperfection theory on an equatorial coupled ocean–atmosphere model, Neelin and Dijkstra (1995) showed that flux correction introduced spurious equilibria in that system. The restrictions placed upon the system by flux correction required it to produce a climate state similar to that observed, regardless of parameters. For parameter values where feedbacks were strong, this led to the production of spurious equilibria instead of the modification of an existing one. Tziperman et al. (1994) have noted sensitivity of multiple equilibria to the restoring timescale used in establishing the flux correction in oceanic general circulation models. Chen and Ghil (1995) comment on the effects of flux correction in thermohaline circulation (THC) variability. In a simple coupled box model of the North Atlantic, Marotzke and Stone (1995) have pointed to specific errors in transient behavior induced by traditional flux-correction procedures. These studies, and the rather drastic consequences of flux correction in the equatorial system, motivate us to examine the impact of a prototype for flux correction in the thermohaline system. In this study, we mimic the correction procedure used in MS88 using a two-dimensional ocean model that captures the occurrence of multiple equilibria. Qualitatively similar effects may be expected under the gentler flux-adjustment procedure proposed by Weaver and Hughes (1996).

We demonstrate that flux correction changes the location of the multiple equilibria in parameter space. Consequently, there exist areas in parameter space

where multiple equilibria exist in the flux-corrected case, but there is a unique state in the true case. By using model–model intercomparison we draw conclusions on the multiple equilibria as determined by MS88, which provide guidelines on how to distinguish spurious from real cases. Although we focus mainly on implications for the MS88 coupled model, these guidelines apply equally well to ocean-only models, which are flux corrected in a similar way: restoring conditions toward observed salinity are used to spin up the ocean. The diagnosed salinity flux is then used in subsequent runs with mixed boundary conditions (Bryan 1986; Marotzke and Willebrand 1991; Weaver and Sarachik 1991; Weaver et al. 1993).

2. Formulation

The model of the thermohaline circulation is similar to that used previously in Cessi and Young (1992), Quon and Ghil (1992), and Thual and McWilliams (1992). Although this model is far from realistic, it represents the thermohaline transport in a clear way and captures the advective feedback responsible for the occurrence of multiple equilibria. A Boussinesq flow model on a two-dimensional pole-to-pole ocean basin of length L and depth H is considered as a model of the zonally averaged thermohaline ocean circulation. The diffusivities of heat κ_T, salt κ_S, and momentum ν, are assumed constant and isotropic and must be interpreted as eddy diffusivities. The governing equations are nondimensionalized using scales H, κ_T/H, ΔT, and ΔS for length, velocity, temperature, and salinity, respectively. Here ΔT, and ΔS are characteristic meridional temperature and salinity differences. A linear equation of state is assumed, with thermal and solutal coefficients indicated by α_T and α_S. With horizontal and vertical velocities v and w, respectively, the governing equations in streamfunction ψ and vorticity ζ (with $v = \partial\psi/\partial z$, $w = -\partial\psi/\partial y$ and $\zeta = \partial w/\partial y - \partial v/\partial z$) formulation are

$$\mathrm{Pr}^{-1}\left(\frac{\partial\zeta}{\partial t} + v\frac{\partial\zeta}{\partial y} + w\frac{\partial\zeta}{\partial z}\right) = \nabla^2\zeta + \mathrm{Ra}\left(\frac{\partial T}{\partial y} - \lambda\frac{\partial S}{\partial y}\right) \tag{1a}$$

$$\zeta = -\nabla^2\psi \tag{1b}$$

$$\frac{\partial T}{\partial t} + v\frac{\partial T}{\partial y} + w\frac{\partial T}{\partial z} = \nabla^2 T \tag{1c}$$

$$\frac{\partial S}{\partial t} + v\frac{\partial S}{\partial y} + w\frac{\partial S}{\partial z} = Le^{-1}\nabla^2 S. \tag{1d}$$

All boundaries are assumed stress free and the lateral and bottom boundary are isolated and impervious to salt, that is,

$$y = 0, A: \psi = \zeta = \frac{\partial S}{\partial y} = \frac{\partial T}{\partial y} = 0 \tag{2a}$$

$$z = 0: \psi = \zeta = \frac{\partial S}{\partial z} = \frac{\partial T}{\partial z} = 0. \tag{2b}$$

At the ocean surface, the usual mixed boundary conditions are prescribed, that is,

$$z = 1: \psi = \zeta = 0, \qquad \frac{\partial T}{\partial z} = -B[T - T_0(y)],$$

$$\frac{\partial S}{\partial z} = \gamma Q_T(y), \tag{2c}$$

where the function T_0 is a prescribed temperature distribution. The thermal boundary condition is a simple Newtonian cooling law with interfacial heat transfer coefficient h. The temperature T_0 is interpreted as an apparent atmospheric equilibrium temperature (Haney 1971). The parameter γ measures the strength of the surface freshwater flux, and Q_T models its spatial structure. When the surface integral of this function is zero, the total steady-state salt content is conserved as either time or parameters are varied. Note that the salinity is determined up to an additive constant in the mixed boundary formulation.

In addition to γ in (2c), the equations above contain six other dimensionless parameters: the Prandtl number Pr, the Lewis number Le, the thermal Rayleigh number Ra, the buoyancy ratio λ, the Biot number B, and the aspect ratio A, defined by

$$\mathrm{Pr} = \frac{\nu}{\kappa_T}, \qquad \mathrm{Le} = \frac{\kappa_T}{\kappa_S}, \qquad \mathrm{Ra} = \frac{g\alpha_T\Delta T H^3}{\nu\kappa_T},$$

$$\lambda = \frac{\alpha_S\Delta S}{\alpha_T\Delta T}, \qquad B = \frac{hH}{\rho C_p\kappa_T}, \qquad A = \frac{L}{H}. \tag{3}$$

In this formulation, it appears that only the product $\sigma = \gamma\lambda$ is an independent parameter that can be shown by rescaling $\tilde{S} = \lambda S$. Hence, apart from parameters appearing in the functions $T_0(y)$ and $Q_T(y)$, the equations form a dynamical system having six parameters (σ, A, Ra, Le, Pr, B). Of these, Ra and σ will be used as control parameters while the other parameters are kept at standard values: Pr = 2.25, Le = 1, A = 10, and B = 100. In Dijkstra and Molemaker (1997) it was shown that the bifurcation diagrams for A = 10 were qualitatively similar to that in the asymptotic limit $A \to \infty$. Since these bifurcation diagrams also remain qualitatively similar in the case of nonisotropic diffusivities (Vellinga 1996), the area in parameter space seems appropriate to study qualitative features of solutions of the thermohaline circulation.

3. Multiple equilibria: True flux versus "corrected" flux

Steady solutions of the governing equations are computed using continuation methods; details of the solution techniques are provided in Dijkstra and Molemaker (1997).

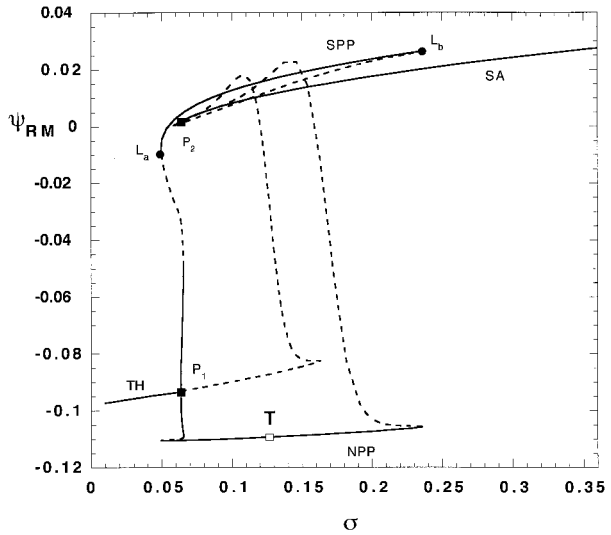

FIG. 1. Bifurcation diagram in σ, the parameter controlling the strength of the salt flux, for the forcing Q_T and T_0 and standard values of other parameters, in particular Ra = 10^4. On the vertical axis, the streamfunction value ψ_{RM} at a grid point in the northern part of the domain and middle depth $y/A = 0.851$, $z = 0.500$ [grid point (45, 15) of the grid] is shown. Solid (dotted) lines indicate stable (unstable) solutions and bifurcation points are indicated by markers. For this measure of the flow, symmetric solutions branches TH and SA may be distinguished from each other. However, pitchfork bifurcations P_1 and P_2 do not appear symmetric, although the solutions for NPP and SPP are mirror images about the equator. The point T denotes the value chosen as the true solution.

a. Solutions without flux correction

The functions $T_0(y)$ and $Q_T(y)$ are chosen as

$$T_0(y) = \frac{1}{2}\left\{\cos\left[2\pi\left(\frac{y}{A} - \frac{1}{2}\right)\right] + 1\right\} \tag{4a}$$

$$Q_T(y) = 3\cos\left[2\pi\left(\frac{y}{A} - \frac{1}{2}\right)\right]. \tag{4b}$$

Under the symmetric forcing (4) and Ra = 10^4, the bifurcation diagram with respect to σ is shown in Fig. 1. This diagram is similar to that presented in Fig. 16 of Dijkstra and Molemaker (1997). For low σ, up to the limit point marked L_a, there is only the thermally driven solution (TH branch). For high σ, above the limit point L_b, there is only the saline-driven solution (SA branch). Between L_a and L_b there are multiple equilibria, since additional northern pole-to-pole (NPP) and southern pole to pole (SPP) solutions are stable.

The northern sinking solution (on the NPP branch) is closest to the observed overturning circulation. To provide a prototype for the flux-correction problem, we choose a point on this branch to be considered as the true solution under the true flux Q_T. In the procedure which follows, ''incorrect'' values of parameters are used to represent model inadequacies that prevent it from obtaining this true NPP solution under the flux Q_T. A correction in the flux is then calculated from solutions under boundary conditions that restore surface variables toward the true solution. When the model is run with this flux-corrected salt flux, it can then reproduce solutions approximating the true solution, despite incorrect parameters. This correction, however, affects not only the NPP branch in Fig. 1 but also the other branches. Their movement in parameter space will be the main point of interest.

We first focus on the point marked T (true) on the NPP branch at $\sigma = 0.128$ in Fig. 1, which will be our prototype for the observations in this model–model study. The flow pattern of this northern sinking solution is shown in Fig. 2a and its temperature and salinity in Figs. 2a and 2c, respectively. In Fig. 2d, the surface salinity of this solution is plotted as a function of latitude. We designate this true surface salinity field as S_T. We will refer to the bifurcation diagram in Fig. 1 as the true structure of the equilibria in the model under the symmetric forcing (4).

Now suppose it is difficult with the model, under conditions (4), to reach the true solution. This may be due, for example, to an underestimation of one of the parameters controlling the strength of the overturning circulation; here we choose the Rayleigh number Ra. This would mimic a situation where correct boundary conditions are used, but the model is run with viscosity and/or diffusivity that are too high compared to the true values. This is a plausible prototype for errors that occur in climate GCMs, and it corresponds to lower Ra than the true value. To show how the solution structure varies in Ra, the branches in Fig. 1 (for fixed $\sigma = 0.128$) are followed in Ra, giving the result in Fig. 3. Contour plots of the streamfunction at marked points along the stable solution branches are shown in Fig. 4. For Ra larger than the value at the limit point L_1, the ocean has multiple equilibria. Hence, this value (5.1×10^3) can be considered critical and is therefore indicated by Ra_c. As was shown in Dijkstra and Molemaker (1997), all bifurcations in Fig. 1 shift to smaller values of σ as Ra is decreased. At the value of Ra_c, the limit point L_b of Fig. 1 has shifted to σ values lower than $\sigma = 0.128$ and the SA solution is the only solution. In physical terms, the model is too viscous or diffusive for poleward advection of salt to be able to maintain the pole-to-pole solutions.

b. Flux-correction procedure

Suppose the value of Ra in the model is smaller than Ra_c. Then, the NPP solution does not exist (Fig. 3) and a saline-driven flow will be obtained for arbitrary initial conditions. Since this circulation does not correspond at all to the true circulation, a correction procedure is introduced to approximate it. Likewise, if Ra is smaller than the true value but larger than Ra_c, the branch of the overturning solution can be reached but will be too weak and a flux correction procedure can be introduced to strengthen it. The procedure in MS88 is as follows:

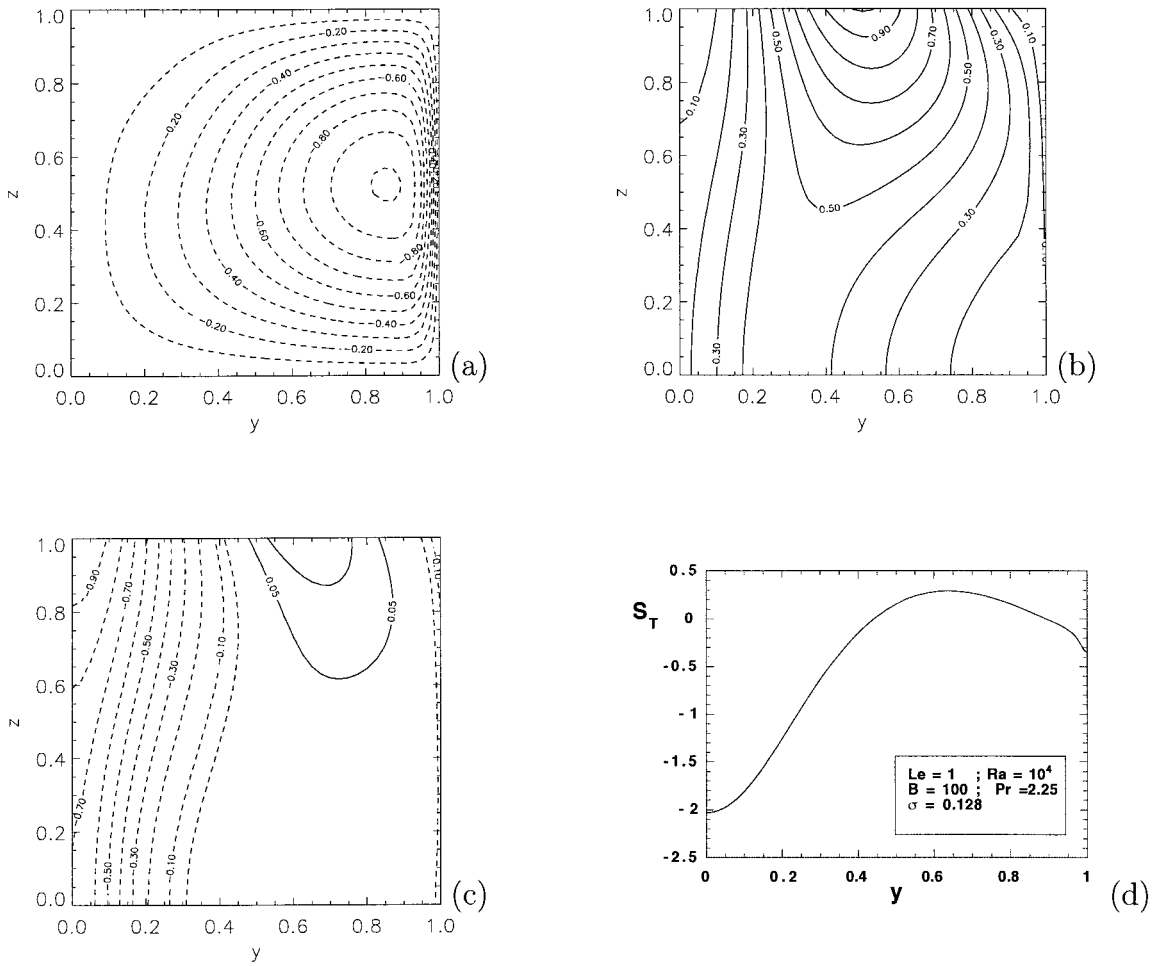

FIG. 2. Solution fields at the point T in Fig. 1: (a) streamfunction ψ, *with maximum* $\psi_m = 0.11$; (b) temperature T, *with maximum* $T_m = 0.98$; and (c) salinity S, *with maximum* $S_m = 2.02$. In the contour plots, each field is scaled by its absolute maximum, ψ_m, T_m, or S_m, and contour levels are with respect to this maximum. Latitude y is scaled by A and north is to the right. (d) Surface salinity.

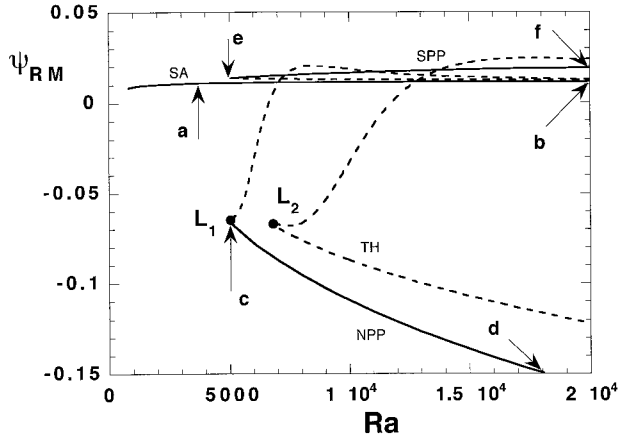

FIG. 3. Bifurcation diagram in Ra for $\sigma = 0.128$ with the forcing Q_T and T_0 and standard values of other parameters. Format as in Fig. 1. Labels a–f indicate points for which solutions are shown in Fig. 4.

first, restoring conditions for salinity using the true salt field S_T are prescribed and the resulting steady state computed. Second, the freshwater flux Q_{FC} at this steady-state solution is diagnosed. Third, the freshwater flux Q_{FC} is used to force the model instead of Q_T. Note that if one applies this procedure at the right value of Ra, exactly the true solution is obtained, since $Q_{FC} = Q_T$.

However, assume that the correction is needed because the value of Ra is too low or too high. To compute the freshwater flux needed to maintain the true surface salinity, we change Ra under the restoring boundary conditions that maintain S_T and monitor the freshwater flux Q_{FC}. Under restoring conditions, it is well known that there is only a single steady-state branch. This branch is shown with varying Ra in Fig. 5, with the point T again indicated at Ra = 10^4. For lower values of Ra the overturning circulation is weaker, as expected for a model with higher viscosity and diffusion. A contour plot of the flux-correction freshwater flux Q_{FC} along

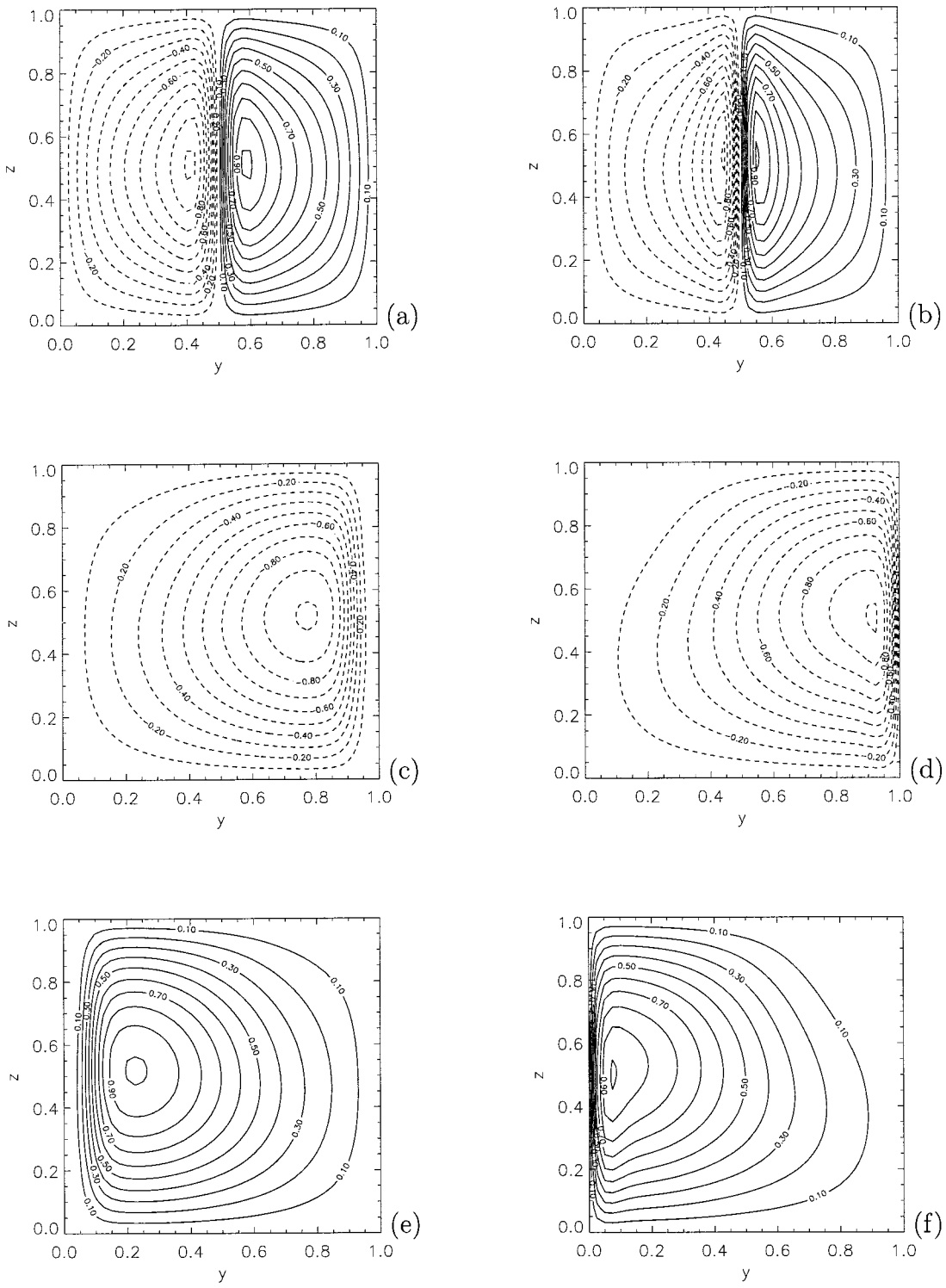

FIG. 4. Patterns of the streamfunction at selected points along the branches shown in Fig. 3. Format as in Fig. 2: (a) $\psi_m = 2.26 \times 10^{-2}$, (b) $\psi_m = 3.45 \times 10^{-2}$, (c) $\psi_m = 7.01 \times 10^{-2}$, (d) $\psi_m = 1.54 \times 10^{-1}$, (e) $\psi_m = 7.01 \times 10^{-2}$, and (f) $\psi_m = 1.74 \times 10^{-1}$.

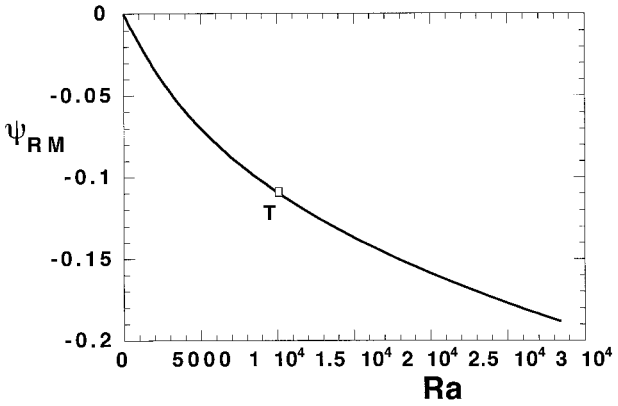

FIG. 5. Bifurcation diagram in Ra for restoring boundary conditions that fix surface salinity and temperature to S_T and T_0 and standard values of parameters with $\sigma = 0.128$. Format as in Fig. 1.

the branch in Fig. 5 is shown in Fig. 6a, with several sections at different Ra in Fig. 6b. At Ra $= 10^4$, the true value of Ra, this flux is symmetric and equal to Q_T. It becomes asymmetric in latitude as Ra $\neq 10^4$ because the true surface salinity field S_T associated with the NPP branch is asymmetric.

As seen in Fig. 6, for larger Ra, the spatial pattern of the freshwater flux required to maintain S_T is not changed dramatically. Larger overturning increases the salt transport to the surface in the southern part of the basin. To maintain the true salt field, the amplitude of the freshwater flux must increase. Moreover, the freshwater flux should increase slightly more in the south relative to the north. For small Ra, the circulation is very small and the salt field can only be established by oceanic diffusion. Hence, the spatial structure of the freshwater flux becomes similar to the true surface salinity field, and its magnitude decreases, since the input required to maintain S_T is small when circulation is weak.

In the third step of flux correction, the freshwater flux Q_{FC}, instead of Q_T, is now prescribed. For any given value of Ra, the corresponding value of Q_{FC} is given that can maintain S_T. However, under mixed boundary conditions, multiple equilibria are possible, so we recompute all solutions.

c. Solutions under flux correction

The bifurcation diagram that occurs under flux correction is shown in Fig. 7. The computation is aided by using a homotopy parameter to continue solution boundaries from the original prescribed flux Q_T to that using the corrected flux Q_{FC}. Since the occurrence of pitchfork bifurcations is connected to the reflection symmetry about the equator, the immediate consequence of the equatorially asymmetric flux Q_{FC} is that the pitchfork bifurcations connecting the SA and TH branches to the NPP and SPP branches no longer exist. A so-called imperfection of the bifurcation diagram has occurred

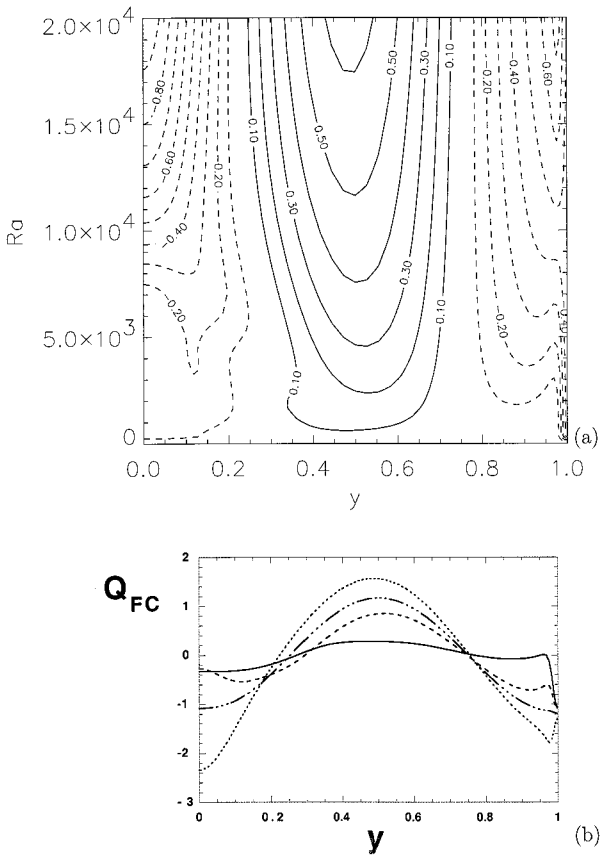

FIG. 6. (a) Contour plot of the flux-correction freshwater flux forcing $Q_{FC}(y)$ as a function of latitude (scaled by domain length) and Ra. This is the flux required to maintain the true surface salinity field S_T, even when model parameters (here only Ra) differ from the true values. The field is scaled by its absolute maximum and contour levels are with respect to this maximum. (b) Sections at different values of Ra, with Ra $= 7.56 \times 10^2$ (solid), Ra $= 5.35 \times 10^3$ (dashed), Ra $= 9.54 \times 10^3$ (dash–dotted), and Ra $= 1.77 \times 10^4$ (dotted).

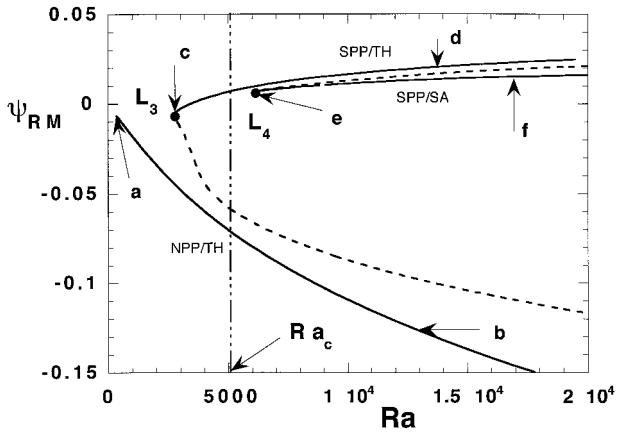

FIG. 7. Bifurcation diagram in Ra for the flux-corrected case: forcing Q_{FC} and T_0 and the standard values of the parameters and $\sigma = 0.128$. Format as in Fig. 1. Labels a–f indicate points for which solutions are shown in Fig. 8.

and the branches reconnect according to known imperfect pitchfork structures (Iooss and Joseph 1981). Contour plots of the streamfunction along the stable branches are presented in Fig. 8. The branch labeled NPP/TH is (by the correction procedure) similar to the branch computed through the restoring boundary conditions (Fig. 5). Hence, even for $Ra < Ra_c$, a northern sinking solution is obtained. When the value of Ra becomes too small, a second cell appears in the southern half of the basin (Fig. 8a) so the circulation differs considerably from the true solution, even though the surface salinity is the same by construction. With sinking at both poles, this resembles the TH branch of Fig. 3. There is a significant interval of Ra around the true values where the NPP/TH branch resembles the true solution (Fig. 8b), although the strength of the circulation varies. So, within this range the flux-correction procedure might be considered successful.

A main point of the results in Fig. 7 is that the other branches in Fig. 3 are drastically modified and their topology is substantially different from that of the true case. The major difference between the solution structure for the true case and the flux-corrected case is the Ra interval of existence of the branches. The NPP/TH branch, a reconnection between the TH and NPP branches, exists down to small Ra in the corrected case, whereas it exists only down to Ra_c in the true case. On the other hand, the SPP/SA branch, a reconnection between the SA and SPP branches, exists only down to $Ra = 6 \times 10^3$, whereas it exists over the whole Ra range in the true case. Hence, under the flux correction, the collapse of the circulation from NPP to SA, which should occur if Ra is too small, is prevented by adding/removing sufficient freshwater at the correct location to maintain the true salinity. The spatial structure of solutions at the SPP/TH branch is also modified by an additional cell with sinking in the north (Fig. 8c) at low Ra in the flux-corrected case. Likewise, at low Ra the SPP/SA branch differs from SA in having a three-cell structure (Fig. 8e), although solutions correspond well at larger Ra (Fig. 8f).

The most important result is that the reconnection between the TH and SPP branches, the SPP/TH branch in Fig. 7, exists down to $Ra = 3 \times 10^3$ in the flux-corrected case, whereas in in the true case (Fig. 3) multiple equilibria do not exist below Ra_c. The unstable TH branch exists down to $Ra = 6.5 \times 10^3$ in the true case, but is modified to connect to the SPP under flux correction. The number of stable solutions, their interval of existence, and their flow patterns for the true and corrected case can be compared in Figs. 3 and 4 and Figs. 8 and 7. In the regime of correct Ra, the number and flow pattern of the solutions correspond well and flux correction does not alter the result on the existence of multiple equilibria. However, one has to be careful in the range of smaller Ra. Below Ra_c, there are now multiple equilibria, which are absent in the true case. In the range between 3×10^3 and Ra_c it is possible in the flux-corrected case to induce a (spurious) transition between a northward sinking solution to a southward sinking solution, for example, by adding a sufficiently large freshwater perturbation in the north. Furthermore, the properties of the branches are substantially modified, likely with attendant changes in the basin of attraction.

4. Discussion

Within one of the simplest models representing thermohaline transport, we have considered the impact of flux correction on the structure of multiple equilibria. The effect is not so strong as in the tropical ocean–atmosphere case (Neelin and Dijkstra 1995), where multiple equilibria were shown to be an artifact of flux correction and completely disappeared in the uncorrected case. In the thermohaline-driven circulation, as modeled here, there is considerable good news. Over a reasonable interval in parameter space, the multiple equilibria of the flux-corrected case and the true case are similar. The flux correction is successful at maintaining a northern sinking NPP branch qualitatively comparable to the true solution even for parameters differing considerably from those of the true case. However, the spatial form of the other equilibria, and the connections between them, may differ noticeably from the true case. Furthermore, there exists an interval in parameter space where the flux correction has artificially introduced multiple equilibria. This effect occurs just in the range of Ra where the model needs a strong correction to resemble the true state under restoring conditions.

In the present model, the reason for the artificial multiple equilibria is the existence of the SPP/TH branch down to the limit point L_3 (Fig. 7) with the simultaneous existence, by construction, of the NPP/TH branch. At Ra slightly smaller than Ra_c, the freshwater flux (Fig. 6) in the south part of the basin exhibits a minimum near the southern end of the basin ($y = 0.1A$). Relatively more salt is put in at the south and consequently the SPP/TH solution can be maintained at smaller Ra than the SPP solution with the true flux.

One might now ask whether the multiple equilibria found by MS88 are indeed artificially induced by their flux-correction procedure. Of course, the coupled model they use is much more complex than the simple model used in this study. However, under the assumption that the structure of the large-scale multiple equilibria is indeed determined by the advective feedback in the ocean and that these carry over to the coupled system as in Saravanan and McWilliams (1995), the structure of the different solutions in MS88 and those in the simple model can be compared.

The data from the MS88 runs have been analyzed in detail in part I of England (1992), where plots of the meridional overturning streamfunction of the Atlantic are also provided. The equilibrium E_1, as referred to in the introduction, clearly resembles the present clima-

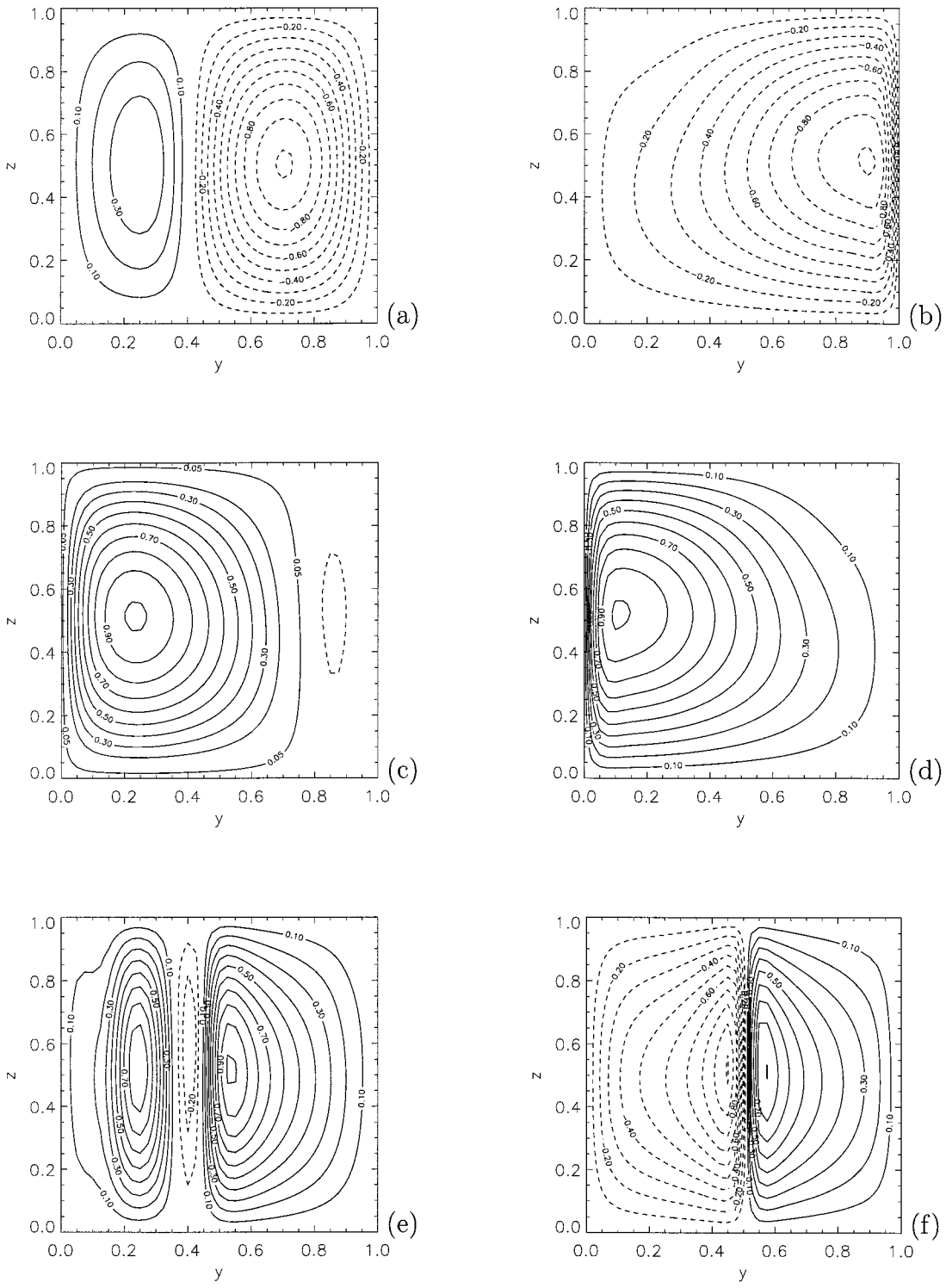

FIG. 8. Patterns of the streamfunction at selected points along the branches shown in Fig. 7. Format as in Fig. 2: (a) $\psi_m = 1.40 \times 10^{-2}$; (b) $\psi_m = 1.39 \times 10^{-1}$; (c) $\psi_m = 5.08 \times 10^{-2}$; (d) $\psi_m = 1.36 \times 10^{-1}$; (e) $\psi_m = 2.41 \times 10^{-2}$; and (f) $\psi_m = 4.48 \times 10^{-2}$.

tology and can be identified with the NPP/TH branch in Fig. 7. The overturning streamfunction for the state E_2 appears negative, from Figs. 8 and 9 in England (1992), over most of the Atlantic and can be identified with the SPP/TH branch rather than the SPP/SA branch. This is also compatible with the differences in salinity and temperature distributions [as shown in Figs. 15 and 16 of part I in England (1992)] of the states E_1 and E_2. In terms of the parameters of our simple model, the value of Ra is larger than that at L_3 (Fig. 7), but it is unclear by how much. By comparing Figs. 3 and 7, one can see the important role of the limit point L_1 (at the value Ra_c) in determining whether the state E_2 in MS88 is spurious; when Ra is smaller (larger) than Ra_c it is (is not) spurious.

To determine the parameter regime of the model, one can look at the state E_p in MS88 (at the end of the uncorrected coupled spinup). This state is characterized by weak overturning and the sea surface salinity is much too low in the North Atlantic (Fig. 5 in MS88). Unfortunately, no overturning streamfunction for this state is presented in MS88 or England (1992) and it is not possible to identify this state either with SA or SPP. If it were an SA-like equilibrium, then this would correspond to a value of Ra in the model smaller than the value at L_1. Under flux correction, the initial conditions for experiment I in MS88 would then correspond to a point near the NPP/TH branch in Fig. 7. In a transient integration a particular point on this branch (the state E_1 in MS88) is reached since the solutions on this branch are stable. The initial conditions for experiment II in MS88 would correspond to a point near the SPP/TH branch in Fig. 7. Under flux correction it would approach this branch and the equilibrium E_2 would be spurious. If the state E_p is a SPP-like state, the value of Ra is larger than the value at L_1, and neither equilibria found in MS88 is induced by flux correction. In summary, while we do not have enough data from the MS88 runs to determine whether the multiple equilibria are spurious, qualitative information from the bifurcation diagram could be used to make informed guesses from the GCM runs.

The results of the analysis indicate that any result on multiple equilibria should be viewed with caution when only flux-corrected models are used. Results of an uncorrected run with the coupled model are important, even though the equilibrium state obtained, for example, E_p, may be far from observations. It can be used to determine the parameter regime of the model, and the state E_p may give more information than the magnitude of the actual correction. In our simple model, Fig. 3 indicates that when the state E_p is an NPP-like state (with perhaps smaller overturning than observations) or an SPP-like state, multiple equilibria exist in both flux-corrected and uncorrected models and have a direct correspondence. In fact, since the interval of existence of the SPP/SA branch (Fig. 7) is smaller in the flux-corrected case than that of the SA branch in the uncorrected case (Fig. 3), if this condition is met then no spurious equilibria arise in the flux-corrected case in this prototype system. The case where spurious equilibria may occur due to flux correction is when the state E_p is an SA-like state. Results of an uncorrected simulation are clearly essential to distinguish the two situations.

To summarize, while there may be many reasons to be concerned about the effects of flux correction on model phenomena, the prototype system here supports cautious use of flux correction for the THC problems, subject to several caveats. (i) The system without flux correction must not be too far from the realistic regime; the smaller the correction the better. (ii) Results for the equilibrium state for which the flux correction is constructed are more reliable than for other equilibria found under this flux correction. (iii) Conclusions regarding multiple equilibria in the flux-corrected system are more likely to be trustworthy if analogous equilibria are found in the uncorrected system, even if the comparison to observations in the uncorrected system is less than desired. This may encourage modelers to document the uncorrected cases more carefully, even if they intend to use flux correction.

Acknowledgments. All computations were performed on the CRAY C98 at the Academic Computing Centre, Amsterdam, the Netherlands, within Project SC498. Use of these computing facilities was sponsored by the Stichting Nationale Supercomputer Faciliteiten (National Computing Facilities Foundation) with financial support from the Netherlands Organization for Scientific Research (NWO). This work was initiated and completed during visits of HD to the University of California, Los Angeles, in 1996 and 1997 and sponsored by NSF Grant ATM-9521389 and an NWO PIONIER grant.

REFERENCES

Broecker, W. S., D. M. Peteet, and D. Rind, 1985: Does the ocean–atmosphere system have more than one stable mode of operation? *Nature*, **315,** 21–26.

Bryan, F., 1986: High-latitude salinity effects and interhemispheric thermohaline circulations. *Nature*, **323,** 301–304.

Cessi, P., and W. R. Young, 1992: Multiple equilibria in two-dimensional thermohaline circulation. *J. Fluid Mech.*, **241,** 291–309.

Chen, F., and M. Ghil, 1995: Interdecadal variability of the thermohaline circulation and high-latitude surface fluxes. *J. Phys. Oceanogr.*, **25,** 2547–2560.

Dijkstra, H. A., and M. J. Molemaker, 1997: Symmetry breaking and overturning oscillations in thermohaline flows. *J. Fluid Mech.*, **331,** 169–198.

England, M. H., 1992: The global-scale circulation and water-mass formation in a World Ocean model. Ph.D. thesis, University of Sydney, 225 pp.

Haney, R. L., 1971: Surface thermal boundary condition for ocean circulation model. *J. Phys. Oceanogr.*, **1,** 241–248.

Iooss, G., and D. D. Joseph, 1981: *Elementary Stability and Bifurcation Theory*. Springer-Verlag, 324 pp.

Lenderink, G., and R. J. Haarsma, 1994: Variability and multiple equilibria of the thermohaline circulation associated with deep-water formation. *J. Phys. Oceanogr.*, **24,** 1480–1493.

Manabe, S., and R. Stouffer, 1988: Two stable equilibria of a coupled ocean–atmosphere model. *Climate Dyn.,* **1,** 841–866.

Marotzke, J., 1994: Ocean models in climate problem. *Ocean Processes in Climate Dynamics: Global and Mediterranean Examples,* P. Malanotte-Rizzoli and A. R. Robinson, Eds., NATO ASI Series C, Vol. 419, Kluwer, 79–109.

——, and J. Willebrand, 1991: Multiple equilibria of the global thermohaline circulation. *J. Phys. Oceanogr.,* **21,** 1372–1385.

——, and P. Stone, 1995: Atmospheric transports, the thermohaline circulation, and flux adjustments in a simple coupled model. *J. Phys. Oceanogr.,* **25,** 1350–1364.

Moore, A. M., and H. B. Gordon, 1994: An investigation of climate drift in a coupled atmosphere–ocean–sea ice model. *Climate Dyn.,* **10,** 81–95.

Neelin, J. D., and H. A. Dijkstra, 1995: Ocean–atmosphere interaction and the tropical climatology. Part I: The dangers of flux correction. *J. Climate,* **8,** 1343–1359.

Quon, C., and M. Ghil, 1992: Multiple equilibria in thermosolutal convection due to salt-flux boundary conditions. *J. Fluid Mech.,* **245,** 449–484.

Rahmstorf, S., 1994: Rapid climate transitions in a coupled ocean–atmosphere model. *Nature,* **372,** 82–85.

Saravanan, R., and J. C. McWilliams, 1995: Multiple equilibria, natural variability, and climate transitions in an idealized ocean–atmosphere model. *J. Climate,* **8,** 2296–2323.

Sausen, R., K. Barthel, and K. Hasselman, 1988: Coupled ocean–atmosphere models with flux-correction. *Climate Dyn.,* **2,** 145–163.

Stommel, H., 1961: Thermohaline convection with two stable regimes of flow. *Tellus,* **2,** 244–230.

Thual, O., and J. C. McWilliams, 1992: The catastrophe structure of thermohaline convection in a two-dimensional fluid model and a comparison with low-order box models. *Geophys. Astrophys. Fluid Dyn.,* **64,** 67–95.

Tziperman, E., J. R. Toggweiler, Y. Feliks, and K. Bryan, 1994: Instability of the thermohaline circulation with respect to mixed boundary conditions: Is it really a problem for realistic models? *J. Phys. Oceanogr.,* **24,** 217–232.

Vellinga, M., 1996: Instability of two-dimensional thermohaline circulation. *J. Phys. Oceanogr.,* **26,** 305–319.

Weaver, A. J., and E. S. Sarachik, 1991: The role of mixed boundary conditions in numerical models of the ocean's climate. *J. Phys. Oceanogr.,* **21,** 1470–1493.

——, and T. M. C. Hughes, 1992: Stability and variability of the thermohaline circulation and its link to climate. *Trends in Physical Oceanography,* Research Trends Series, Vol. 1, Council of Scientific Research Integration, 15–70.

——, and ——, 1996: On the incompatibility of ocean and atmosphere models and the need for flux adjustments. *Climate Dyn.,* **12,** 141–70.

——, J. Marotzke, P. F. Cummings, and E. S. Sarachik, 1993: Stability and variability of the thermohaline circulation. *J. Phys. Oceanogr.,* **23,** 39–60.

Zhang, S., R. J. Greatbatch, and C. A. Lin, 1993: A reexamination of the polar halocline catastrophe and implications for coupled ocean–atmosphere modeling. *J. Phys. Oceanogr.,* **23,** 287–299.